NUMERICAL SIMULATION OF OPTICAL DIFFRACTION RADIATION FROM A 7-GEV BEAM*

C.-Y. Yao†, A. H. Lumpkin, D. W. Rule‡
Advanced Photon Source, Argonne National Laboratory, Argonne, IL 60439, U.S.A.

Abstract

Experimental study and numerical modeling have been performed on the optical diffraction radiation (ODR) of the 7-GeV beam of the Advanced Photon Source (APS) booster-to-storage ring (BTS) transport line. This report describes the simulation method, the results, and the comparison with experiment results.

INTRODUCTION

Interest in nonintercepting (NI) beam size monitoring for top-up operations at the Advanced Photon Source (APS) motivated our investigations of optical diffraction radiation (ODR) techniques. We have reported our experimental results elsewhere [1]. In particular, we wanted to monitor the beam size in the booster-to-storage ring (BTS) transport line using near-field ODR. An analytical model was numerically evaluated for the APS BTS beam size cases. In addition, the simulations show that near-field ODR profiles have sensitivity to beam size in the 20- to 50-μm region, which are relevant to the APS ERL Upgrade, x-ray FELs, and the International Linear Collider (ILC). The simulation indicates that the perpendicular polarization component is close to a Gaussian distribution and more sensitive to beam-size variations, and therefore is more suitable for beam-size measurement. Under some circumstances the parallel polarization component shows a non-Gaussian distribution that is also beam-size dependent.

NUMERICAL INTEGRATION

Numerical modeling of the ODR radiation produced by a 7-GeV electron beam on the ODR plate of the APS BTS beam transfer line was performed. Figure 1 shows a sketch of the screen configuration with an impact parameter (IP) of b.

The analytical model we adopted for the simulation is based on the method of virtual quanta described by Jackson [2] for relativistic beams.

The basic idea is that virtual photons moving with a charged particle interact with the atoms in the ODR plate and produce scattered photons. The differential ODR field intensity for a relativistic Gaussian beam can be expressed as [1]:

$$\frac{dI}{d\omega}(u,\omega) = \frac{1}{\pi^2}\frac{q^2}{c}\alpha^2 N \frac{1}{\sqrt{(2\pi\sigma_x^2)}}\frac{1}{\sqrt{(2\pi\sigma_y^2)}} \times \iint dx\,dy\,K_1^2(\alpha b)e^{-x^2/2\sigma_x^2}e^{-y^2/2\sigma_y^2}, \quad (1)$$

where ω is radiation frequency, c is the speed of light, q is the electron charge, N is the number of particles, **u** = (u_x, u_y) is the coordinate of the observation point, **b**=**u**-**r** is the distance between the particle and observation point, α=2π/(γλ), and K_1 is the first modified Bessel function. The integration is performed over the entire beam distribution area with rms spatial dimensions of σ_x and σ_y. In practice, an area covering several beam size is sufficient.

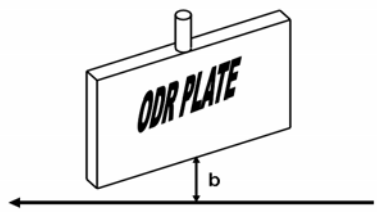

Figure 1: ODR experiment setup.

Figure 2 shows the geometry viewed from the beam direction. The center of the beam is chosen as the origin of the coordinate, **r** is the location of individual particle, and **u** is the observation point where ODR is to be evaluated. A square mesh was generated over a 3-σ area around the beam center, and an integration program was written using the SDDS Toolkit [3]. Detailed discussion of our virtual photon approach to calculating ODR is given in [4].

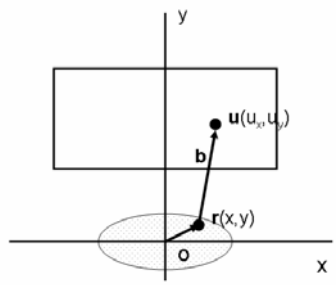

Figure 2: The geometry for the simulation. **u** is the observation point of ODR radiation. **r** is the location of an electron of the beam. The shaded area represents the passing beam.

* Work supported by U.S. Department of Energy, Office of Science, Office of Basic Energy Sciences, under Contract No. DEAC02-06CH11357.
† cyao@aps.anl.gov
‡ Member of Carderock Division, NSWC, West Bethesda, MD 20817, U.S.A.

COMPARISON WITH EXPERIMENT

Figure 3 shows a measured image of the unpolarized ODR light and a plot of the simulated result for a beam with 1375 μm × 200 μm beam size and an IP b=1.25 mm. The simulation showed clear dependence of half width half multitude (HWHM) on the beam width. We varied the IP b from 1.0 mm to 4.0 mm and found there was a 12% change in HWHM of unpolarized ODR profile. This variation can be easily offset by a fit algorithm or a look-up table, in practical applications.

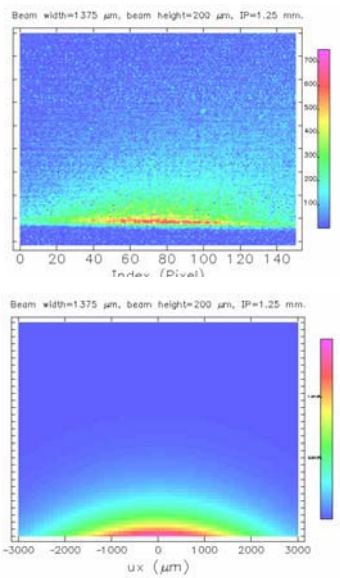

Figure 3: Measured (top) and simulated (bottom) unpolarized ODR intensity contours.

POLARIZED ODR RADIATION

The polarized component of differential ODR is expressed as:

$$\frac{dI}{d\omega}(u,\omega) = \frac{1}{\pi^2}\frac{q^2}{c}\alpha^2 N \frac{1}{\sqrt{(2\pi\sigma_x^2)}}\frac{1}{\sqrt{(2\pi\sigma_y^2)}}$$

$$\times \iint \frac{(u_x - x)^2}{(u_x - x)^2 + (u_y - y)^2} dx\, dy\, K_1^2(\alpha b) e^{-x^2/2\sigma_x^2} e^{-y^2/2\sigma_y^2}. \quad (2)$$

Here only the parallel polarization component, i.e. parallel to x-direction of Fig. 2, is shown; the perpendicular component has similar expression. We decided to simulate the polarized ODR with small beam sizes, which is of interest to future accelerators.

The simulation results of polarized ODR radiation in the beam size range of 20 to 100 μm showed that the radiation distributions in parallel and perpendicular polarizations are very different. Figure 4 shows the two distribution profiles together with the unpolarized ODR profile. The parallel polarization profile has a double peak feature with a minimum at $u_x = 0$. This is the direct result of a single-particle ODR profile. The unperturbed radiation field of a relativistic particle has only radial electrical field, which does not have parallel polarization component along the u_x=0 line. For large beam size this feature is smeared out by convolution. We also found that as the IP increases, the feature becomes weaker. The parallel polarized radiation is a factor of two weaker than the vertical. On the other hand, the perpendicular polarization profile has smaller spread than that of the total intensity profile and is better suited for beam size measurement. This is shown in Figure 4 as well.

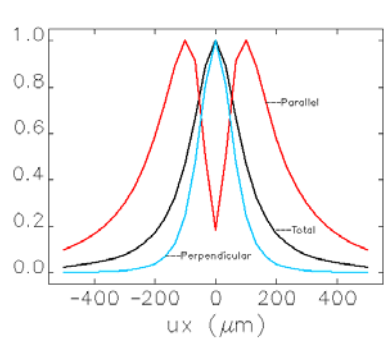

Figure 4: Comparison of different ODR polarization. Red: parallel polarized. Aqua: perpendicular polarized. Black: total intensity. The intensity scales are normalized for convenience. Gaussian beam width is 20 μm and height is 20 μm. IP b = 100 μm.

Figure 5 shows the perpendicular polarization profile for the 20-, 35-, 50- and 100-μm cases. It is clear that there is a strong dependence of the calculated horizontal half width on the horizontal beam size.

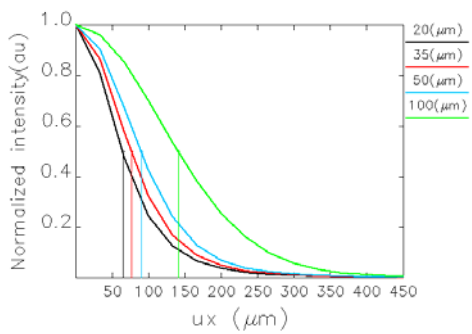

Figure 5: Analytical model results for the effects on the orthogonal polarized ODR horizontal profiles for variation of the beam widths from 20 μm to 100 μm and a constant beam height of 20 μm. IP b=100 μm. Legend is beam width in μm.

For the parallel polarized component the effect of beam width appears in the depth of the valley between the two peaks. In principle this can also be exploited for beam width measurement. Figure 6 shows a dependence of the parallel polarized profiles on the beam widths. Figure 7 shows the relationship between the ratio of the ODR intensity at $u_x = 0$ and the peak intensity and the beam widths. Under 100 μm there is a strong dependence.

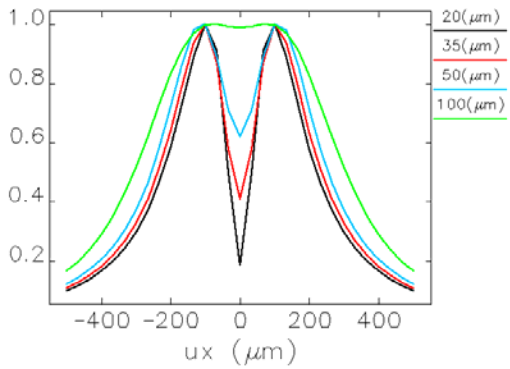

Figure 6: Simulated parallel ODR profile for IP of 100 μm and different horizontal beam sizes. Legend shows beam size.

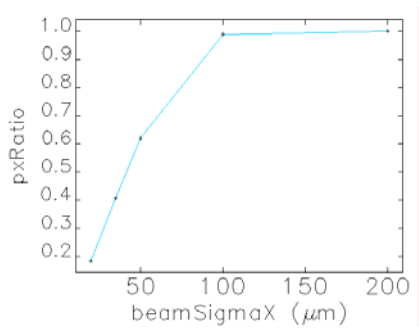

Figure 7: Ratio of parallel ODR intensity at u_x=0 and the peak intensity for different beam sizes. Note that above 100 μm the double peak disappears and the ratio is always 1. At beam sizes below 100 μm, the ratio has beam size dependency.

EFFECT OF IMPACT PARAMETER

The impact parameter is directly related to energy exchange between the incident beam and the ODR plate. It has direct affect on the measured ODR profile.

Our simulation shows a near-linear relation between the HWHM perpendicular ODR radiation distribution and the Gaussian beam width when the IP is between 1 to 6 times the vertical beam size. A linear fit produced the following simple relationship:

$$w_h(b,\sigma_x) = -21.62 + 1.2106\sigma_x + 0.6125b - 0.00164b\sigma_x \quad (3)$$

where w_h is the ODR HWHM width, b is the IP, and σ_x is the beam width of the Gaussian distribution.

However, the intensity of the ODR decreases with IP exponentially with a scale length of α, Eq. (1). This implies that when applying ODR to nonintercepting beam size detection, one has to set the distance between the beam and the ODR plate to a range of a few beam heights. If the distance is too small, the tail of the incident beam will hit the plate directly and produce OTR contamination. Too large a distance will make the ODR intensity too low. It is necessary to stabilize the beam orbit with orbit feedback so that the IP can be maintained consistently.

For a flat beam, which has large beam width and small beam height, it is necessary to maintain a large IP to minimize the OTR contamination. This may result in an unwanted reduction of ODR intensity. In this sense ODR is best suited for round beam applications such as FELs, linear colliders, and ERL beams.

SUMMARY

In summary, we report the result of polarized and unpolarized near-field ODR simulation results using the virtual quanta model. The results are in qualitative agreement with the experiment measurement results at the APS BTS beam transport line. Our simulation results have indicated that perpendicular polarization ODR is effective for the beam size measurement down to a few tens of μm. The parallel polarized ODR can also be used to measure beam size with a different algorithm. These are particularly relevant for such application areas as APS the ERL Upgrade, x-ray FELs, and ILC projects.

ACKNOWLEGEMENTS

The authors acknowledge N. Sereno for his help with the ODR measurements. We also acknowledge M. Borland for his input on the application of the SDDS Toolkit.

REFERENCES

[1] A. Lumpkin, W. Berg, N. Sereno, D. Rule, C. Yao, "Near-field imaging of optical diffraction radiation generated by a 7-GeV electron beam," PRST-Accelerators and Beams, 10, 022802 (2007).

[2] J. D. Jackson, Classical Electrodynamics, John Wiley and Sons, New York, 1975, Sec. 15.4.

[3] M. Borland, L. Emery, H. Shang, B. Soliday, "User's Guide for SDDS Toolkit Version 1.30," http://www.aps.anl.gov/Accelerator_Systems_Division/Operations_Analysis/oagSoftware.shtml.

[4] R. B. Fiorito and D. W. Rule, "Diffraction radiation diagnostics for moderate to high energy charged particle beams," NIMB 173, 67-82 (2001).

